TITLE: Telescope Simulator optical design

DISTRIBUTION

D Smith   (RAL)
B Swinyard   (RAL)
M Caldwell   (RAL)
T Grundy   (RAL)
M Ferlet   (RAL)

CHANGE RECORD

ISSUE	SECTION	REASON FOR CHANGE
1.0		

CONTENTS

Annex 5. Details of simulator bench layout.

1. Introduction.

The purpose of the simulator is to provide a point-source beam at the instrument, of the form close to that from the Herschel telescope. This beam is one which is focused on the instrument FP surface, at the required f-number (8.7), and with a pupil distance equal to that of the telescope (approx. 2.4 metres, diameter ~ 300mm). The design concept is to use a single imaging optic as shown in fig.1, to produce the required pupil as a virtual image of a real stop, in order to save space as compared to using a real pupil. This concept was used for a UKIRT simulator (ref.1). For simplicity the imaging is made 1-to-1.
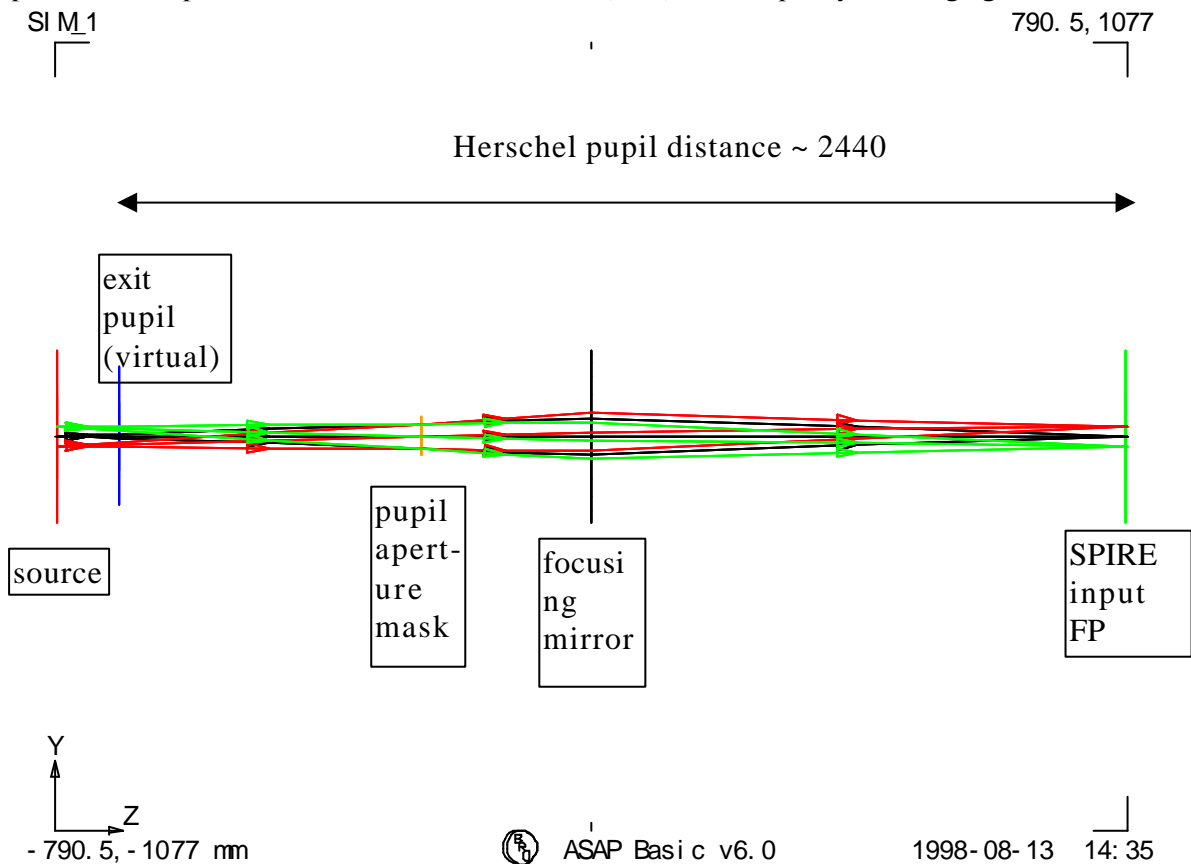
Fig.1. Simulator 1st-order layout, dimensions of plot window are as given at bottom-left & top-right corners (total length approx. 2 metres) Ray-trace is for geometric beam over used FOV.

Figure 1 shows a simulator used with an array of point sources, i.e. a finite FOV range, in order to show the pupil imagery. In practise, however, the need to keep the point-source aberration free over the SPIRE FOV range, and to keep the simulator imaging simple, leads to a design in which only one point source is imaged, and the FOV is mapped by scanning this beam after the imaging mirror.

In this scheme 3 fold mirrors are needed, and for an all-reflective implementation of the system of fig.1, we have a scheme as per fig.2. Here the imaging mirror is an ellipsoid with 90-degree turn angle, providing nominally perfect point source imaging.
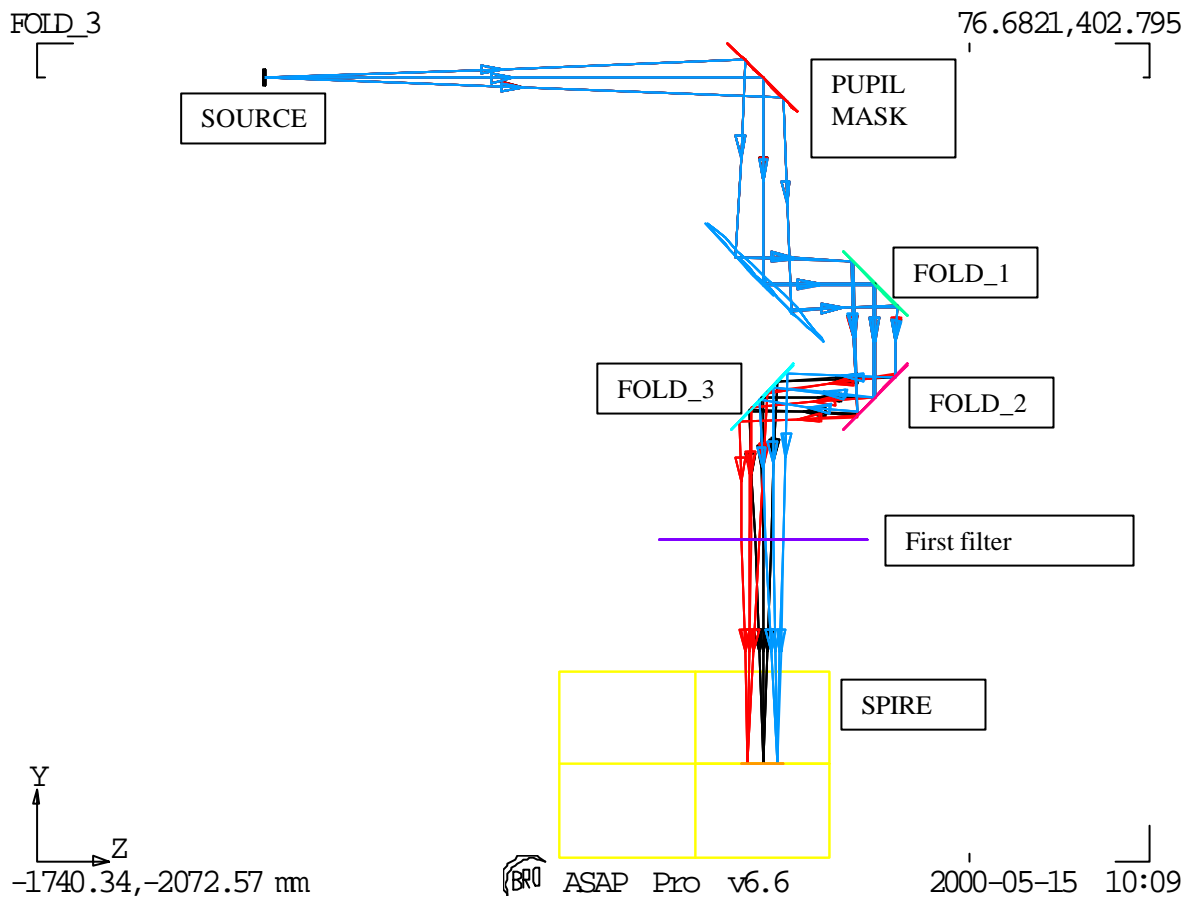
Fig.2. All-reflective design. Input point source shown in blue. The FOV scanning produces output beam also at FOV positions such as those shown in red & black.

Since the beam steering is all done after both the mask & the focusing mirror, so no changes in beam shape or aberration arise with scanning.

2. Simulator sizing.

Following ref.1, for accurate scaling in the representation of the larger (far-field) Herschel pupil the minimum beam dimension must be kept >> wavelength, to maintain the far-field approximation.
This dimension is the diameter D_{M1} of the mask's obscuration, & here we use N>>1 wavelengths, giving

$$D_{M1}=N*\lambda/OBSC$$

Where OBSC is the telescope obscuration factor, given by ratio of FIRST mirror sizes: D_{SM}/D_{PM} = 308.3/3280.2, and λ=0.6mm.

The distance of the mask M1 from the source is

$$L_{M1}=D_{M1}*FNO$$

SPIRE

Technical Note

Ref: SPIRE-RAL-NOT-000 622
Issue: Draft Issue 1.0
Date: 08-05-2001
Page: 5 of 35

(FNO=8.7)

And the required wavefront ROC produced by the 1:1 imaging mirror M2 is

$$R_{SM}=2*L_{M1}*L_{PUP}/(L_{M1}+L_{PUP})$$

$$L_{pup} = (D_{SM}/2)\char94 2/(2*ROC_{SM})+1587.868+1050.162$$

L_{PUP} is the pupil distance to be simulated (i.e. telescope system on-axis exit pupil position), and the 1st term in L_{PUP} is the approx. sag of the secondary mirror. For precise control L_{PUP} is later replaced by the off-axis position L'_{PUP} (section 3.2).

The parameter R_{SM} sets the overall size of the system. Note that the sizing may be changed by using imaging other than 1:1, but then a different FNO is required in the source.

The above figures give R_{SM} ~ 2000 mm, and to give an idea of scale the above simulator layout is shown overlaid with the Herschel telescope in fig.3. below.
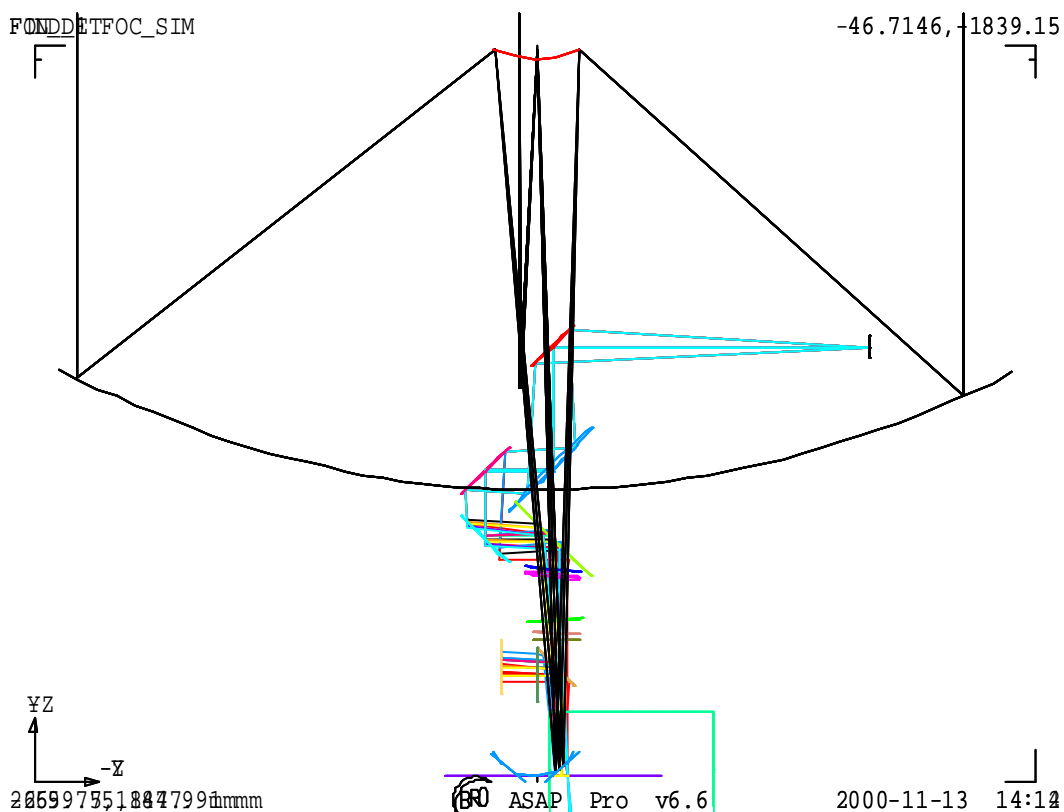
Fig.3. Simulator + Herschel systems.

The imaging mirror needed for this scheme has been investigated, to determine whether toroid or ellipsoid shape is preferred from the viewpoints of beam quality (aberration) requirement, alignment & manufacturing, and the size & spec. of this mirror. This study is reported in ref.4, and the conclusion is that an ellipsoidal shape is needed. Due to the large size this mirror cannot be made smooth & accurate enough to provide optical-quality imaging in the visible region. As a result the mirror verification & the

SPIRE

Technical Note

Ref:	SPIRE-RAL-NOT-000 622
Issue:	Draft Issue 1.0
Date:	08-05-2001
Page:	6 of 35

alignment procedure will have to rely only on mechanical metrology, fiducial marks & small areas of mirror polished. Also the simulator self-verification (of focus & steering control) will have to be performed at the SPIRE test wavelength (i.e. in FIR) ideally using e.g. a Golay cell detector, rather than with a visible trace beam as originally planned.

3. Simulator (scanned) FOV.

The simulator is required to cover the whole SPIRE instrument FOV without the need to re-configure any of the hardware within the cryostat.

The SPIRE geometric FOV is shown in the figure below.
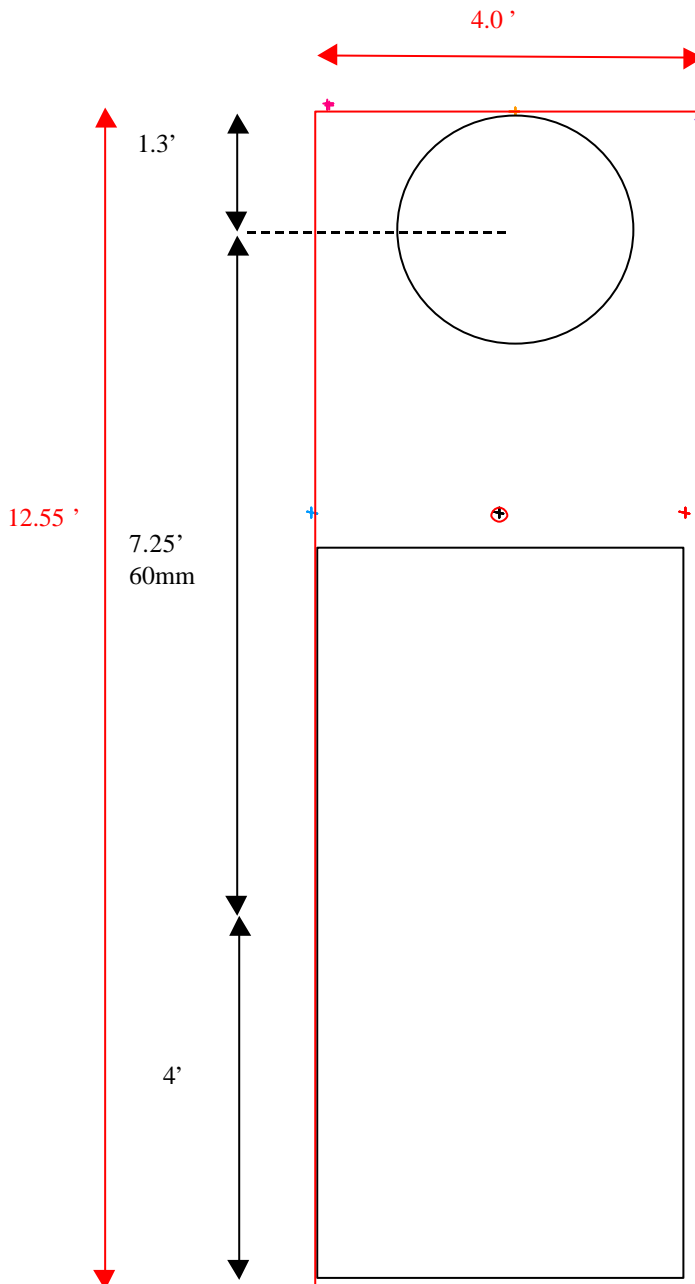
Fig.4. FOV simulator minimum FOV required is shown in red.

4. Spire co-ordinate references.

The off-axis location of the SPIRE FOV within the telescope FOV is by 11 arcmin, leading to 90mm offset of the SPIRE FP from the telescope symmetry axis, as shown in the fig. below.
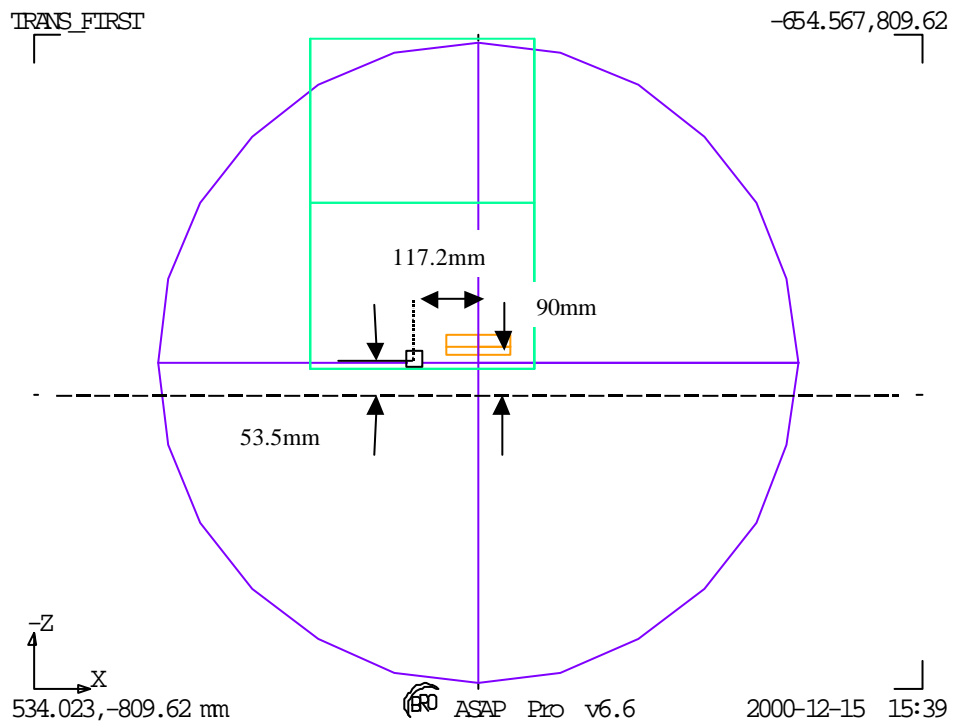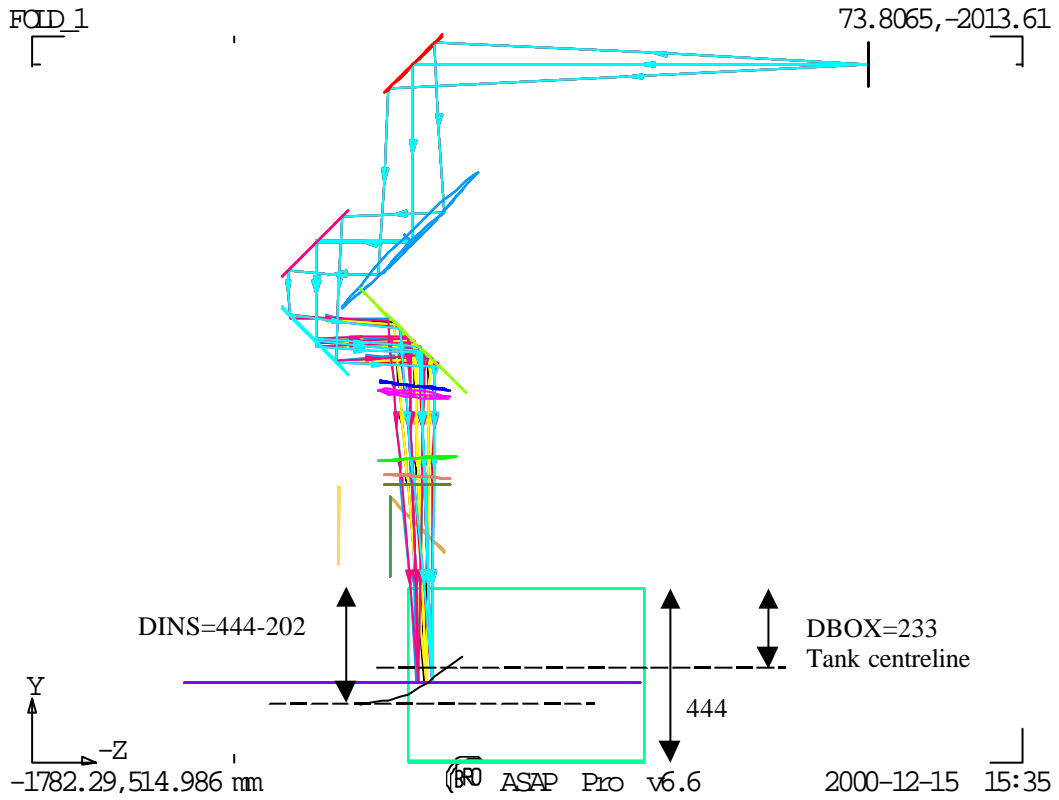
Fig.5. Spire co-ordinates system. Update firsim6.igs FOV=12.55X4 arcmin (maximum)
The figure also shows the SPIRE alignment cube position, taken from drawing MSSL 5264 (ref.2, TBC). This shows the line of sight to the cube to be $\sqrt{(117.2^2+[90-53.5]^2)} = 112.75$mm.

The global co-ordinate system used in the SPIRE optical design also has the telescope symmetry axis as one of its axes (ref.3).

The FP (parabolic surface) radius of curvature is 167.17mm (from JPL design), leading to a focus 'sag' of 24.23mm at the ~ -90mm off-axis position. For the Herschel telescope Cassegrain design, the radius of curvature is 165mm, which leads to a correction of 24.55mm.

5. Cryostat internal items.

The design of filter & black body geometry are detailed in annexes 2 & 3. The latest design, which has been checked with the CAD design of the cryostat is file FIRSIM8.igs, shown in the figure below (it includes the correction due to the parabolic shape of the TFP surface).
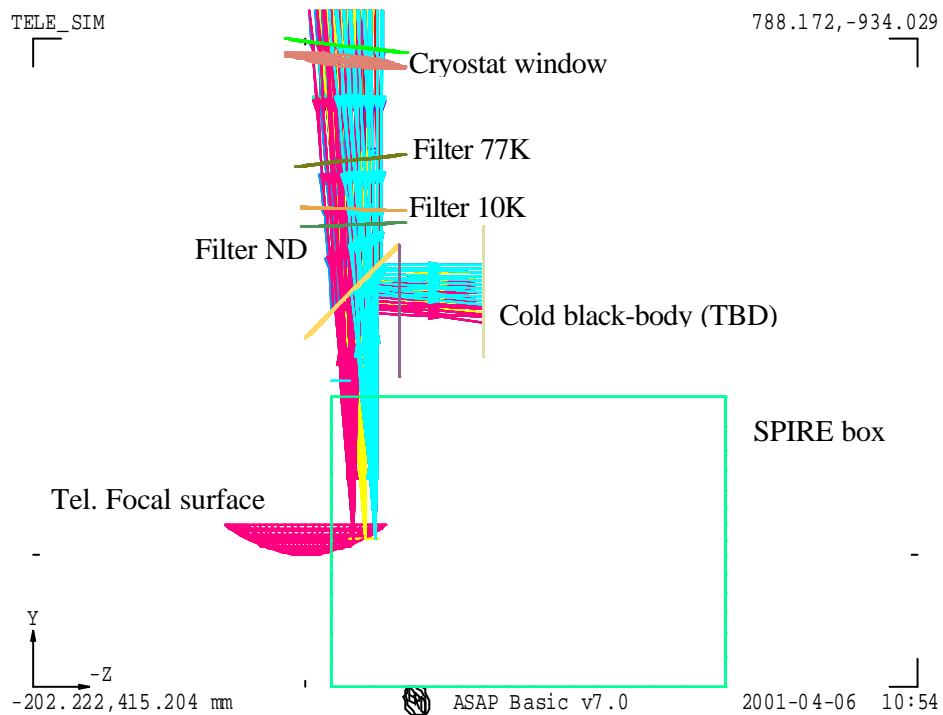
Fig.6. Cryostat internal layout for current design FIRSIM8.igs.

The filter positions have been set to fit the cryostat design and the angles have been re-optimised for anti-ghosting.

5.1. Filter sizes.
The minimum clear aperture required at each filter or window surface is calculated as shown in fig.2 below. The dimensions shown are given in the table & are used to derive the clear aperture diameter (including 20% beam oversize).
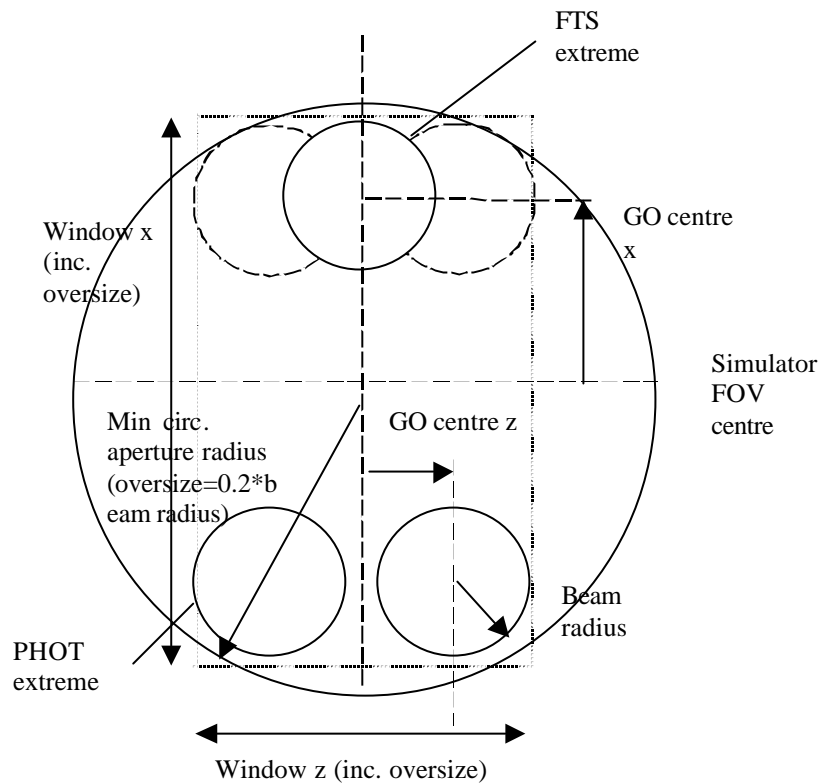
Fig.7. Geometry for calculating minimum clear circular aperture.

The resulting beam footprints are given in the appendix (see Annex 2).

semi-ape z	separation from last surface (dist. y)	beam radius	required diameter 2R	Window x dim.	Window z dim.	surface name
15.23	217.74	12.72	128.40	125.97	60.99	box apert. (SPIRE)
13.56	260.06	27.92	154.35	152.20	94.12	ND filter
13.49	24.92	29.38	156.86	154.70	97.49	10K filter
12.81	75.10	33.76	164.38	162.36	106.66	77K filter
12.47	151.54	42.62	179.69	177.62	127.22	window inner
12.12	22.32	43.92	181.84	179.87	129.66	window outer

6. Simulator & sources bench layout.

The first-cut layout is shown below (Fig. 8), taking up an area of approx. 2.5 x 3.5 metres, whereas the space constraint is closer to ~1x2.5 metres. Due to this, scheme to reduce the overall simulator system size by varying R_{SM} is investigated and detailed in Annex 5.

TRANS_FIRST   3627.09,-2846.84
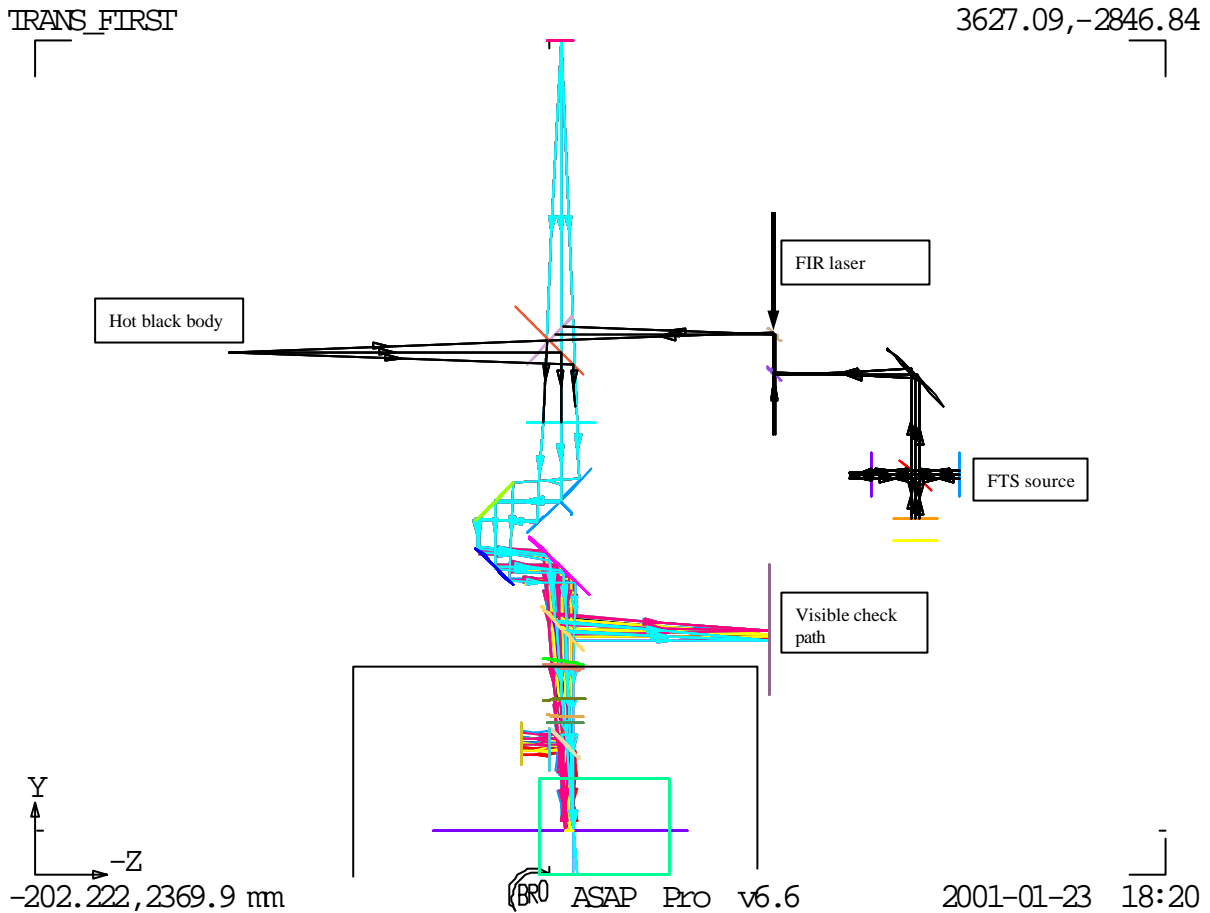
Fig.8. General system layout including sources

In addition the beam height at the cryostat is ~833mm from lab floor, and due to large size of components (imaging mirror, fold mirrors + mounting system), the optical bench may have to be no higher than ~620mm from floor, which is significantly lower than the FIR laser bench (~820 mm).

Figure 9 next page takes these heights into account as well as the space taken by the different sources needed (FTS, hot blackbody). For alignment purpose, a visible laser with reference pinhole R would need to be located at R_{SM} distance from the imaging mirror and in direct view - therefore F1 would be removed and the FTS system can be accommodated in place of the hot blackbody - source in order to define location of the required sources H_1 and H_2. H_3 can be also considered as a source point for the system although realising it as one of the foci of the imaging mirror would require more measurements included in the vertical direction. Details are given in following section. And to keep the FIR laser bench system independent, it can be considered as a provider of a collimated beam which can be injected, after re-shaping by reflective or refractive telescope (to compensate for the beam diffractive divergence over metre or more of free space propagation), into the simulator system as one of the two other points H1 or H2 in replacement of the other sources system.

TELE_SIM

3629.57,-1960.06

FIR laser

CO_2 laser

~1000 mm

H_3

~600 mm

~3000 mm

Base plate with
visible laser for
alignment
(distance H_0-imaging

H_1

R

H_2

~1100 mm

Hot blackbody box

Alternative path for
FIR laser input in the

Cryostat
(low temp.

Y

−Z

−202.222,3260.06 mm

ASAP Basic v7.0

2001-04-26 10:32

FIR laser, system input
height h~100-150mm

Beam in
cryostat
h~833mm

Simulator
bench
h~620mm

FIR laser
bench
h~820mm

Cryolab floor

Fig. 9. *Top (Plan view):* Layout including the FIR laser table with a possible position for a collimated beam output (system parameters: R_{SM}=1980 mm, DF1F2=250 mm, DF2F3=350 mm with a horizontal separation set to 600 mm between the 2 tables and correction, along Y, for sag. of telescope focal surface). *Bottom (Side view):* same system; the height difference (~200mm) between the 2 optical benches is better displayed in this view.

7. Pupil-scanned source.

Another function to be performed by the telescope simulator is the scan of a point source across the pupil as another way of characterising the SPIRE instrument and also to determine the pupil actually seen from SPIRE. The preferred layout including the features required for such a scan is displayed in fig below.
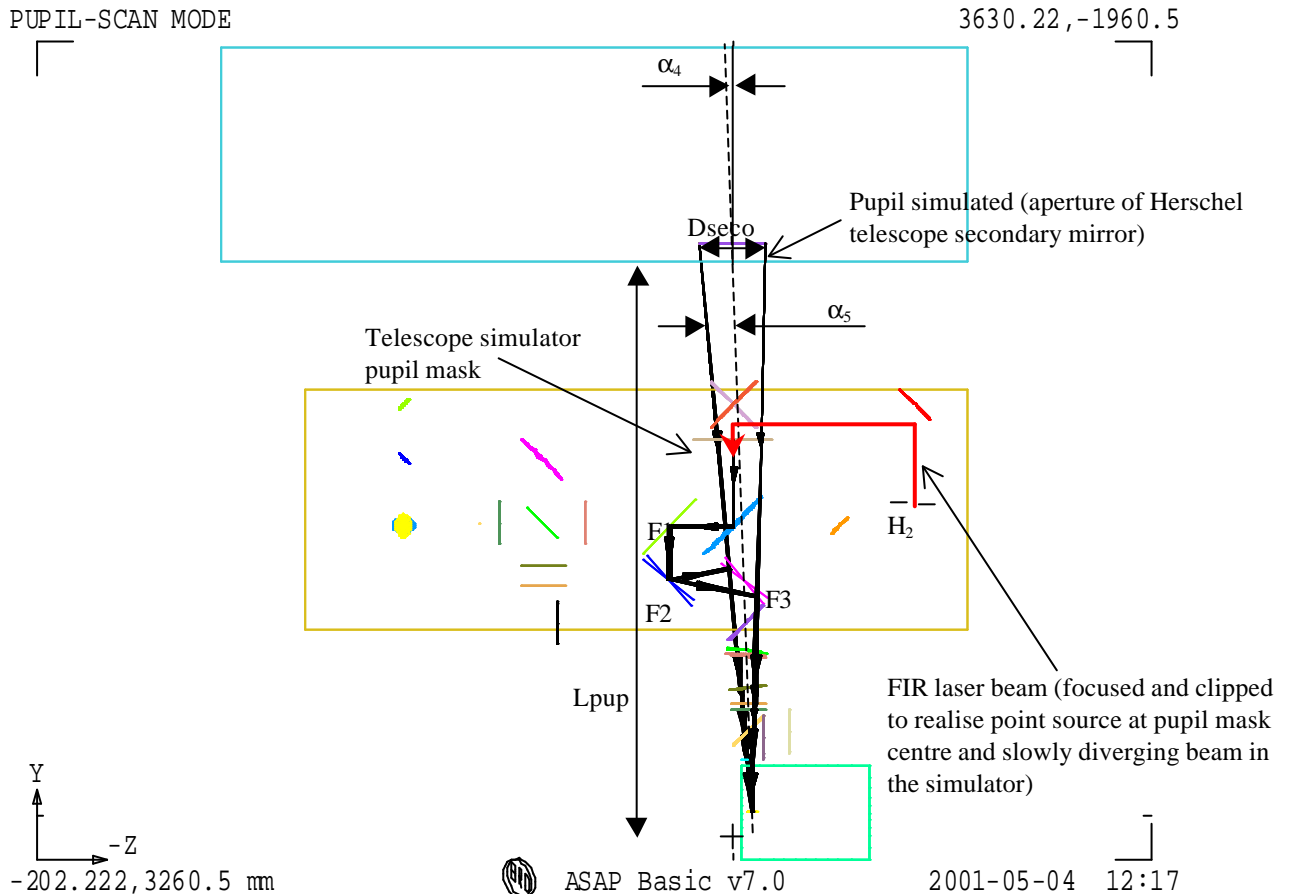
Fig. 10. Telescope simulator layout (plan view). Positions for F2 & F3 are shown after required coupled rotations of both mirrors to simulate a scan across the Herschel Telescope pupil.

This scheme would not require extra actuators as F2 & F3 are already designed to be rotated about their centres and the vertical X-axis in the FOV scanning mode of the simulator. But the range in degrees (see derivation of maximum rotation angles below) would be larger than the ±4.0 deg range, so the actuators would have to be modified in order to perform these larger movements.

No extra translation stage is needed (contrary to what one would expect for a scan across the pupil mask). The point source is created in the centre of the pupil mask from a focused FIR laser which would have been clipped before in order to match the SPIRE field-of-view when propagating on-axis through the entire simulator (fold mirrors in nominal positions). Instrumental effects due to vignetting/clipping by limited size (constraint of space & cost) of the simulator reflective optical components would then be reduced.

- Max. range of rotation required for F2 & F3:

SPIRE

Technical Note

Ref:	SPIRE-RAL-NOT-000 622
Issue:	Draft Issue 1.0
Date:	08-05-2001
Page:	13 of 35

The beam after reflecting on F2 should be angularly displaced by θ_2 to be understood as coming from the edges of the pupil and θ_2 is given by:

$$?_2 = \pm \text{atan}(\frac{P_{F3}}{D_{F2F3} - P_{F3}}) \mp a_4 \text{ with } P_{F3} = \tan(a_{5\_MAX}).D_{F3FP} \text{ and}$$

$$a_{5\_MAX} = \text{atan}(\frac{D_{SECO}/2 - Z_{POS\_SPIRE}}{L_{PUP} - Y_{POS\_SPIRE}}) - a_4 \approx \text{atan}(\frac{D_{SECO}/2}{L_{PUP}})$$

The beam after F3 should be steered by $?_3 = ?_2 \mp a_5$. Finally the mirrors rotation angles are given by $\theta_2/2 \sim \pm 5.2$ deg and $\theta_3/2 \sim \pm 6.8$ deg for F2 and F3 respectively (the $\pm$ symbol stands for the 2 extreme positions simulated at the edge of the pupil although simulating a scan beyond these limits would be useful in their determination).

The above angle ranges apply to a horizontal pupil-scan only. To include the vertical pupil scan would imply a similar increase in the ranges of the vertical adjusters, and due to the 45-degree compound angles involved, these are already approx. $\sqrt{2}$ times larger than in the horizontal. Therefore the vertical case max range may be estimated as $\pm 1.4*6.8 = \pm 9.5$ degrees.

Alternative scheme

In the case where the extra angular range needed for the mirrors prevents the above scheme from being adopted, there is an alternative scheme drawn in the figure below.

This scheme is to fold SPIRE's view through exactly 90 degrees, using a large plane mirror in the position of F3. Unlike F3 this mirror would not be scanned, and it would have to have its angle accurately referenced to the simulator system (e.g. to the bench surface, using e.g. the pentaprism method), in order that the reference of the simulator main path to SPIRE can be maintained.
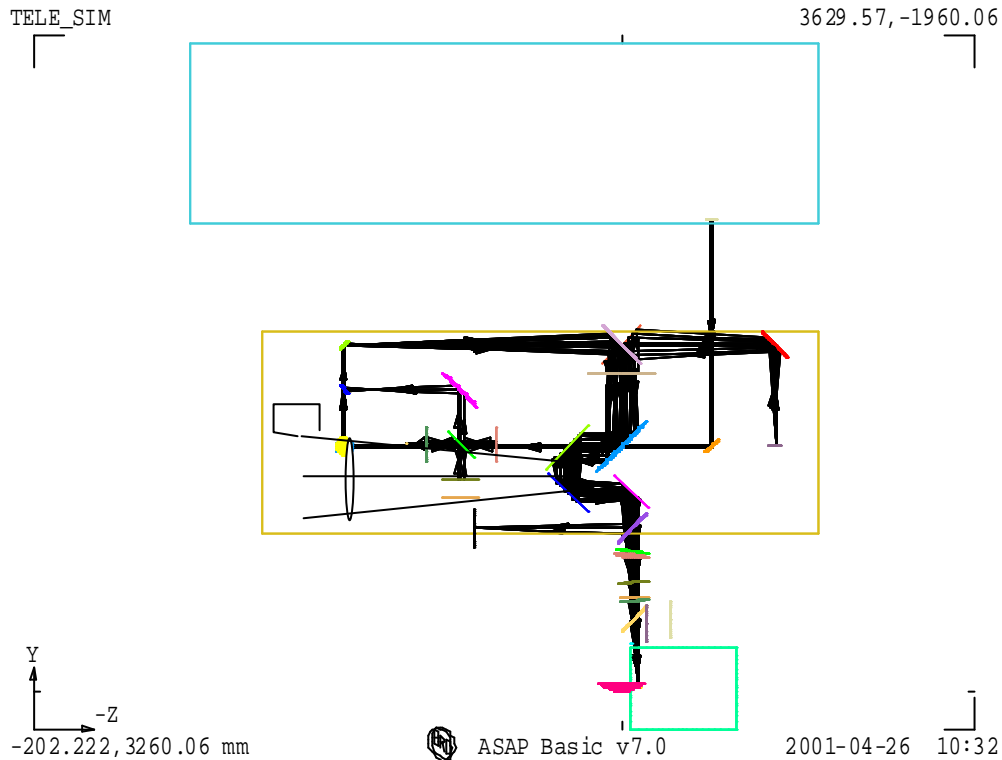
Fig. 11. Telescope simulator layout (plan view). Possible position for the pupil to be scanned (system F1+F2 to be removed, leaving only F3 between SPIRE and the pupil).

The scheme would require both an angle and position control in combination. If dedicated actuators can not be provided, there is the possibility to use the existing actuators from the main path set-up (as these aren't used during this test), but this assumes that those actuators can be easily re-deployed, and it would obviously take extra time to re-configure the system in this way.

The attraction of this scheme is that the SPIRE entrance pupil is then placed in the long direction of the bench, not far from where the nominal path FIR laser beam is focused (when mirrors F1 & F2 are removed). This beam has relative aperture more than adequate for the pupil scan. The simulator focus (H) would need to be relayed to the pupil position, and a collimation+focus arrangement of 2 short-focal length paraboloids could do this. There is then also the capability to add an aperture in the collimated section whose image in the final focus mirror is placed 2.6 metres after the pupil, i.e. correctly at the SPIRE FP, (as is done also in the previous scheme). For example, a focal length of 12cm & SPIRE FP size of 100 x 30mm, this would have size (120/2600) smaller, i.e. 4.6 x 1.4 mm.

The main advantage of this scheme over the preferred one is that it requires smaller angular action; the main disadvantage is that it requires re-deployment of actual actuators or else additional actuators (cf. the nominal imaging-mode set-up).

8. Verification of SPIRE alignment (on QM).

This function of the simulator is to meet the 4 tests required in R5-5. They must be done with the instrument cold, and so with this facility.

The tests involve checks that the alignment of SPIRE both in field position (line-of-sight) and pupil position remain within budget between room & operational temperatures. The tests apply to changes due to both the motion of the whole SPIRE instrument (the SPIRE S-bench) relative to its mounting interface on HERSCHEL (F-bench), and motion of internal components relative to the S-bench (ref: optical error budget, LOOM.KD.SPIRE.2000.002-draft).

The tests can be made on the structural model and so in a separate & earlier cryogenic run to the main calibration task. The tests are in field & pupil positions only, and do not need to include focus, as adequate focus control is ensured by the optical tolerance budget.

The tests are found to be difficult to achieve due to the restriction on using FIR wavelengths to probe at cold temperatures (see below). It is therefore worth considering what requirement lies behind the specific measurements.

Any misalignment in field position places the SPIRE line-of-sight away from its nominal position within HERSCHEL field of view. This impacts the WFE performance and also the astrometric (pointing) calibration.

Any misalignment in pupil position impacts mainly the signal throughput (aperture efficiency), but also the angular response (point spread function). Since the simulator is in any case designed to characterise these aspects, it may appear that pupil position alignment could be tested by the nominal measurement of these parameters in the cold case, i.e. if efficiency & spatial response are in spec. then the pupil position must be OK. The (spurious) effect of changes in F-bench angle (pupil position) with cool down should not affect such a test, as this effect is taken into account in the setting up of the simulator (see section 9).

It may be worth re-considering the worst-case analysis of the impact of the above alignment effects on the mission, to see if there is room to de-scope the more difficult alignment verification tests.

8.1. Pupil alignment.

The requirement is to show:
1. Relative angle motion of S-bench to F-bench is by less than 1 arcmin (0.75mm at herschel pupil, $\Delta R/R = 0.25$ %).
2. Relative position motion of instrument cold stops to S-bench is by <0.1mm (at instrument cold stop, $\Delta R/R \sim 0.1mm/20mm, = 0.5$ %).

The **S-bench to F-bench** is to be done by means of alignment cubes mounted on the SPIRE interface plane (dummy F-bench) and on SPIRE (shown in the above figure), (S-bench). The scheme is shown in the figure below.

FIR probe beam, collimated

Filter flanges & alignment-mode filters

SPIRE (S-bench)

Interface plane (F-bench
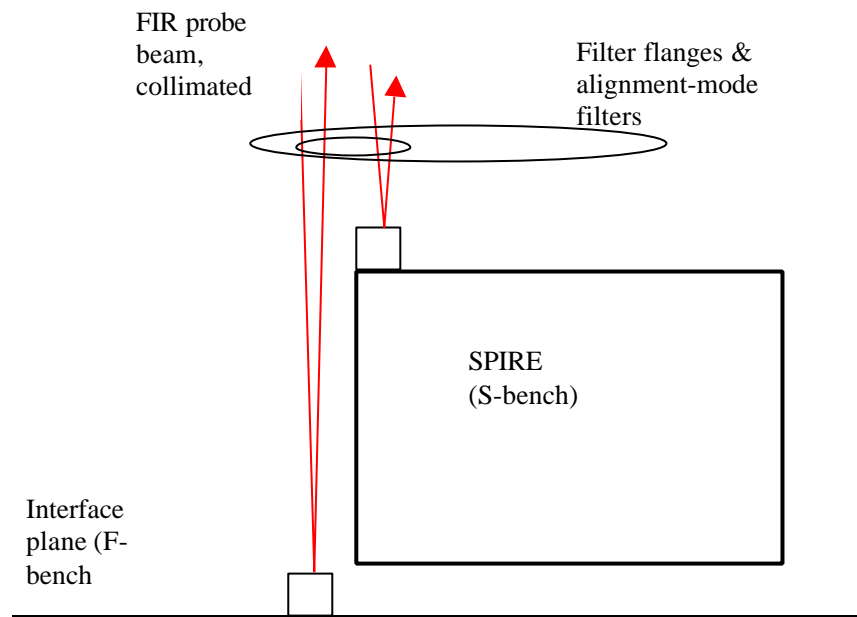
The relative alignment of these cubes is monitored at room T & then at cold T, to detect any changes.

The cold T requires the presence of thermal blocking filters. The nominal filters are sized to just cover the SPIRE FOV, and do not allow access to the SPIRE cube or the interface plane, so a different set of filters will be needed for the alignment tests. The filters will require that a FIR wavelength is needed to probe the cubes. This gives rise to an angular resolution problem since for the usable beam size of ~ 10mm, and min FIR wavelength ~ 0.2mm, the diffraction limited divergence is ~ 0.2/10 = 1.1 degrees. This is much larger than the required angle sensing which is for $\Delta R/R$ =0.7%, equivalent to ~ 4 arcmin. A related problem is that the interface plane is far from the SPIRE cube in the beam direction, so that the size of the 2 returned beams is different. This problem could be overcome by mounting the F-bench reference cube on the frame near the SPIRE cube (this also helps the position test, see below), but then any effects of distortion in the frame would not be detectable in the test.

The diffraction problem would be overcome if the filter responses could allow some much shorter wavelength to be used, e.g. a CO_2 laser near 10μm.

The principle of the test is to locate the retro-reflections from each cube at room temperature, to cool the instrument & to re-locate the reflections, then to determine the change in *relative* angles of the two reflections.

For the **internal angle** changes a scheme is needed for sensing position motion of the cold stop. The most practical way to do this is via the pupil-source operating mode of the simulator (section 9). In this case the detected signal is monitored while scanning bright source across the simulator mask (with the mask absent). The best source for the test is most likely the FIR laser. This produces a map of the beam shape at the pupil. The position of the edges of this beam with respect to the simulator axis shows how well the simulator is aligned to SPIRE. The size & shape of the beam shows (with respect to the model response) whether internal pupil shifts have occurred to level that is significant in causing vignetting. This test requires access to the SPIRE entrance aperture & so needs the nominal filter set; it could not be done in the same cryogenic run as the above test.

8.2 Field position.

The requirement is to show that:
1. Position motion of S-bench to F-bench is by < 0.1mm (impacts LOS budget).
2. Position motion within instrument (defined e.g. by centre detector) in object space relative to S-bench is < 1 arcmin (~2 pixels in PSW).

The **S-bench to F-bench** motion of the instrument would use in the visible the 'fiducial' marks on SPIRE & the interface plane, and view these using an alignment telescope. However, with the restriction to FIR wavelength the equivalent method is to use feedhorn detectors as reference markers. To see the relative motion from room-T to cold these detectors would have to be operable at room-T, and so if possible the CO_2 laser solution would be attractive.

Two such detectors would need to be added, as shown in the figure below. Ideally this test would be done in the same cryogenic run as the above tests. It could use the focused beam from the simulator, but again this would require that the F-bench detector be at a similar range position to the SPIRE detector.

The test would be made in a similar manner to the pupil S-bench to F-bench alignment test, and in this case would require the precise scanning of the test beam between the two detectors while reading them out. The scanning would need to be provided by the simulator, and the filter sizes would need to be larger than for the pupil alignment test.

For the **internal** position motion test, the SPIRE array detector could be used, in a similar scheme to that in 6.1, as shown in the figure below.

FIR probe
beam

Filter flanges &
nominal filters

SPIRE
(S-bench)

Image of centre
SW detector at
SPIRE FP surface

SPIRE

Technical Note

Ref:	SPIRE-RAL-NOT-000 622
Issue:	Draft Issue 1.0
Date:	08-05-2001
Page:	18 of 35
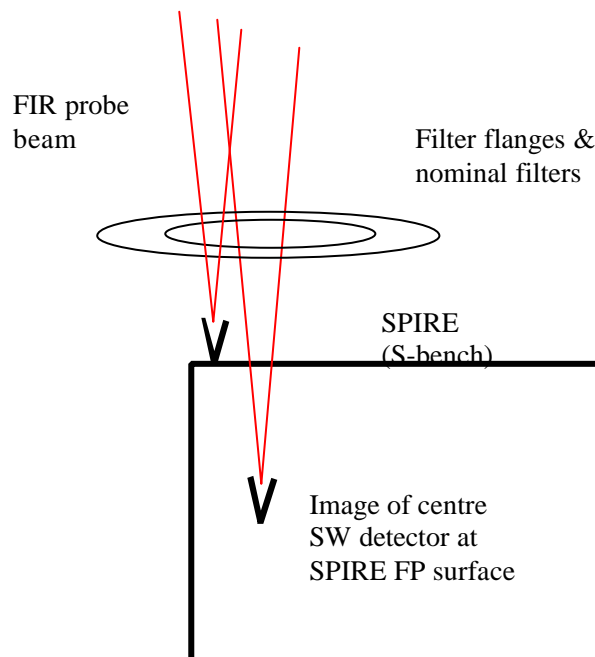
In this case it is desirable that the S-bench detector be located where it is accessible through the nominal simulator filters, as shown above.

The principal of the test is the same as previously, with the added complication that the focus position has to be changed as well as the lateral position. Although the difference in focus positions is large at ~ 20cm, use might be made of the large depth-of-focus of the F/9 test beam at long wavelength, as well as the feature that only relative changes (between room & cold T's) need to be detected.

9. Setting up the simulator (on QM)

The alignment of simulator optics has to ensure that:

1. Reference pinhole apertures 'H' are positioned sufficiently close to the imaging mirror input focus such that when the sources are sent through them they are imaged with low aberration (WFE).
2. The source+mirror system is correctly positioned with respect to the **cold** instrument such that the mirror output beam has:
(a) Focus position 'S', at the nominally centred beam steering position, sufficiently close to the SPIRE FOV centre at the input FP surface (this is needed to ensure that the range of beam steering & focus is sufficient to cover the required range);
(b) Simulator exit pupil position sufficiently close to instrument entrance pupil location (in $\Delta R/R$ terms) for the simulator beam to be representative of the HERSCHEL beam.

To meet the requirement (1) within the above-restricted available space, an alignment procedure has been devised which uses a reverse-direction laser trace beam through a reference pinhole R (at mirror focus). R is permanently set relative to the mirror centre O, and the laser sent through R & O back towards the source references H. In this way the correct source positions can always be referenced correctly & quickly, regardless of how much folding is needed in the input paths & how often it is required to switch between sources.

To meet requirement (2a), the relative positioning of simulator to cold SPIRE, the only option is to make a best nominal position of the simulator before cooling the QM. This should be done using a dummy FP surface with fiducial marks, viewed via the simulator (as per the LWS scheme). As long as the motion on cooling is within the SPIRE fov angle range (±1.5 times 3 cm at the FP, plus similar amount of scan-able range), the simulator beam signal should be sensed e.g. on the p/SW array, and the FOV position error measured in 2 axes. The simulator focus adjustment can then be exercised to determine simulator's focus error (simulator position error in the 3rd axis). The data so derived can then be used to move the simulator (moving O & R together on same baseplate, followed by re-positioning of H), before re-checking. In this way the simulator in its centre-range state is centred up on SPIRE using the QM, and neither cryostat nor simulator mirror focus r are then moved until arrival of the flight model.

For the requirement (2b), simulator pupil position, the SPIRE alignment cube could be use as per the instrument alignment tests. However this requires the different set of filters to the requirement (2a), and so the pupil-source scan is preferred to allow (2a & 2b) to be verified simultaneously. This involves executing the scan of a source across the simulator mask, to determine whether the instrument pupil response map appears centred on the simulator axis (mask position). Having measured the pupil offset in this way it can be corrected by again moving the simulator. To respect the results of the test for (2a), the motion would be a rotation about the output focus position, and detailed metrology will be required to

manoeuvre the simulator into position on the QM with respect to both requirements (2a & 2b) simultaneously.

10. Reference documents:

1. "Long wavelength (sub-mm) telescope simulator", W. Duncan et al., Infra-red Phys. Vol.34, No.1, pp.1-15 (1993).
2. MSSL interface drawing 5264: ISS.1.
3. SPIRE config. Spec04 & Phot03 .xls files.
4. SPIRE-RAL-NOT-000 621, "Design of the Telescope Simulator imaging mirror", M Ferlet (23-03-01).

Annex 1. Telescope simulator control laws.

The figure below is to show the parameters used to set up the ray-trace model above.
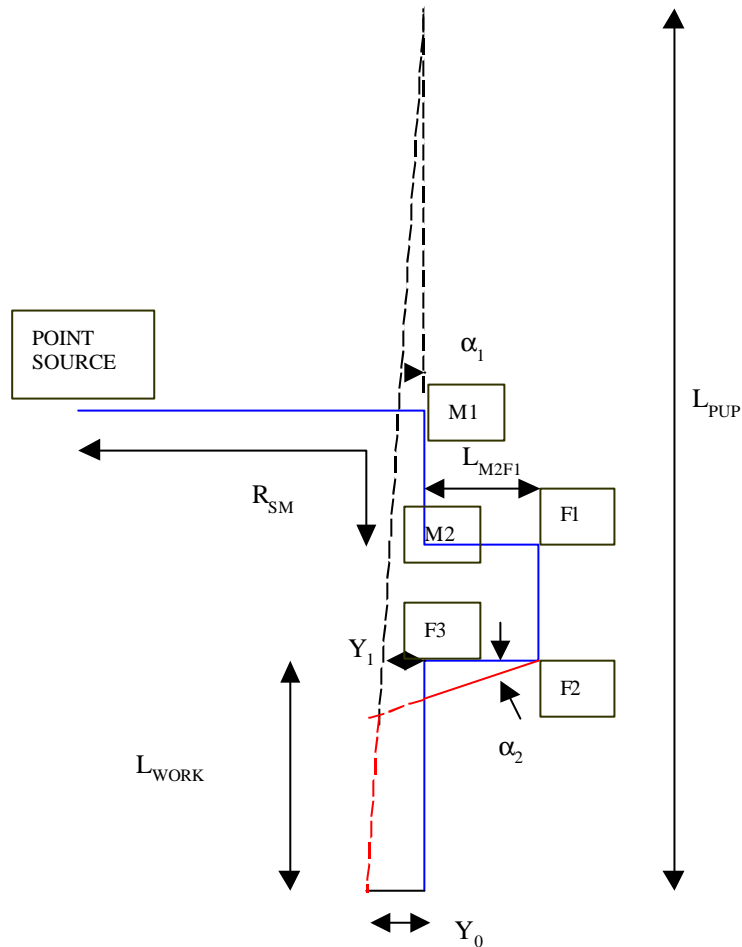
Parameterised layout of fig.1 to show the control-laws.

In the figure the path of the optic axis is shown in blue for centre of SPIRE fov & in red for the edge, i.e. as per fig.1.

3.1 **Control of beam for fov.**
In plane of diagram.
The steering in angle & position are made by combined 'walking' of F2 & F3 to generate the correct output pupil.

The 2nd fold mirror F2 is moved anti-clockwise through angle α_2 /2 , and the 3rd mirror F3 also anti-clockwise, by α_3 /2.

To first order (I,e. for small fov angle α_1):
$$Y_0 = \text{fov\_rad}*F_{TEL}$$
$$\alpha_1 = Y_0/L_{PUP}$$

where fov_rad is the required field of view radius (4 arcmins), F_{TEL} is the telescope focal length (28.5m), L_{PUP} is the secondary mirror to SPIRE input focal point.

Dimension Y_1 is given by

$$Y_1 = \alpha_1.(L_{PUP}-L_{WORK})$$

And

$$\alpha_2 = Y_1/L_{F2F3}$$

$$\alpha_3 = \alpha_2 - \alpha_1$$

in the small-angle approximation, where L_{F2F3} is the distance from mirror F2 to mirror F3.

In fig.1. L_{F2F3} = 250mm, the same for the other fold mirror separations, adequate for handling the beam size at 45 degree incidence.

$$L_{WORK} = R_{SM} - (L_{M2F1}+L_{F1F2}+L_{F2F3})$$

To generate the FOV in the other axis, i.e. that perpendicular to the plane of the diagram (X-axis), to 1st order the same angles α_2 α_3 are used, but are for this case rotations about the Y-axis.

3.2 Focus control.
In plane of diagram.

The correct, non-planer focal surface for SPIRE (not shown in ray-trace fig.1.) would be generated by additionally translating fold_1 & fold_2 on the 'trombone' arrangement.

SPIRE

Technical Note

Ref:	SPIRE-RAL-NOT-000 622
Issue:	Draft Issue 1.0
Date:	08-05-2001
Page:	23 of 35
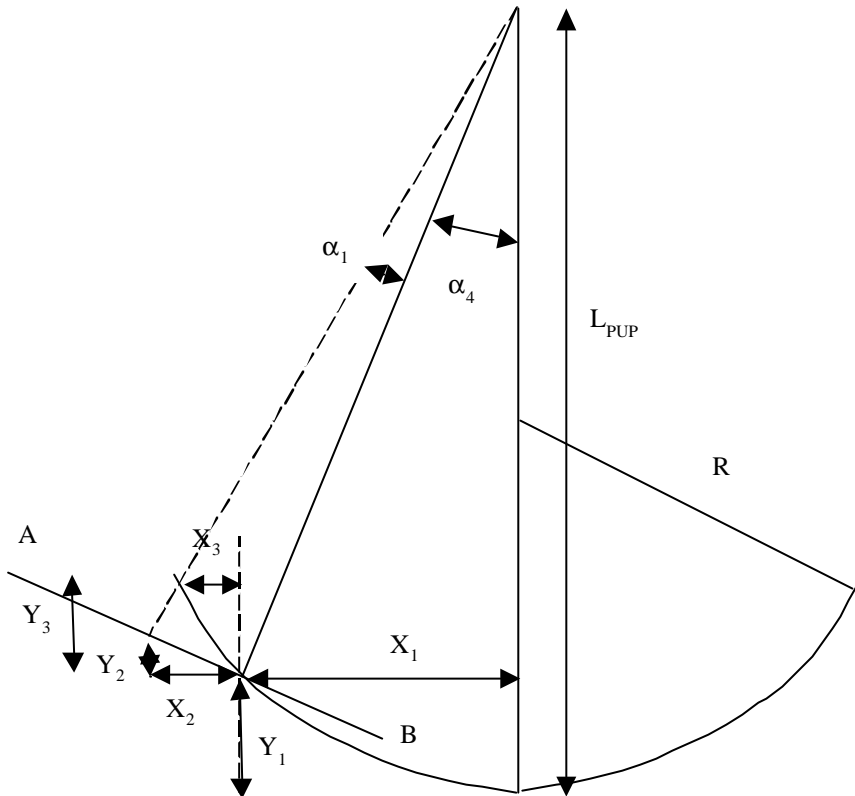
Equation of focal surface:

$$Y_1 = R.(1 - \sqrt{[1-(X_1/R)^2]}) \text{ for a spherical surface approximation}$$

$$\text{or } Y_1 = X_1^2/2R \text{ for the parabolic focal surface}$$

$$X_1 = \tan.\alpha_4.(L_{PUP} - Y_1)$$

α_4 is SPIRE's off-axis position, given by

$$\alpha_4 = \text{fov\_pos}*(F_{TEL}/L_{PUP})$$

where fov_pos = 11 arcmins.

The equations for X_1, Y_1 are solved simultaneously.

At fov angle α_1 (as per fig.2), the co-ords are:

For plane AB:

$$\text{Tan}.\alpha_1 = \Delta l/L'_{PUP}$$

Where Δl is the distance along AB, given by

SPIRE

Technical Note

Ref:	SPIRE-RAL-NOT-000 622
Issue:	Draft Issue 1.0
Date:	08-05-2001
Page:	24 of 35

$$\text{Cos}.\alpha_4 = X_2/\Delta l$$

And $L'_{PUP} = \sqrt{[(L_{PUP}-Y_1)^2 + X_1^2]}$

Together this gives:

$$X_2 = \sqrt{[(L_{PUP}-Y_1)^2 + X_1^2]}. \text{Cos}.\alpha_4. \text{Tan}.\alpha_1$$

$$Y_2 = \tan.\alpha_4.X_2$$

Sphere.

$$Y_3+Y_1 = R.(1- \sqrt{[1-(\{X_1+X_3\}/R)^2]})$$

(or $Y_3+Y_1 = (X_1+X_3)^2/2R$ for paraboloid surface)

$$X_3 +X_1 = \tan.\{\alpha_4 + \alpha_1\}.[L_{PUP}-(Y_3 + Y_1)]$$

Solve for X_3 , Y_3

Focal correction required $= -\sqrt{[(X_2-X_3)^2 + (Y_2-Y_3)^2]}$

In addition, there is already a focal curvature of radius L'_{PUP}, i.e. by sag amount

$$\sim - \Delta l^2/(2.L'_{PUP})$$

To reach the correct focal surface, the F1 + F2 trombone arrangement should be moved to the *right in the figures* by ½ of the difference, i.e. a distance:

$$[\sqrt{[(X_2-X_3)^2 + (Y_2-Y_3)^2]} - \Delta l^2/(2.L'_{PUP})]/2$$

again this is correct only for small-angle changes, i.e. those which give small total variation in path lengths around the 45-degree mirror arrangement.

3a. Alternative scheme.
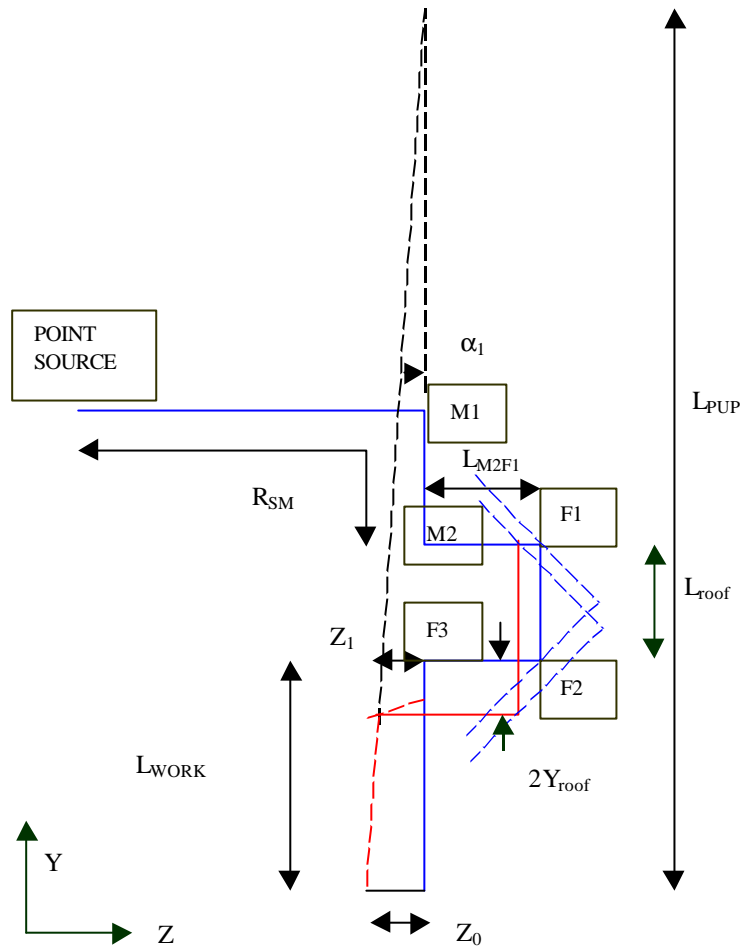
In the figure above, the path of the optic axis is shown in blue for centre of SPIRE fov & in red for the edge, i.e. as per fig.1.

In this scheme, mirrors F1 & F2 are on a common mount, & are e.g. a roof-top mirror, which is moved as a unit. It is moved linear in Y for Z-fov position control, rotated about Z for X-fov position control, and moved linear in Z for focus control. The advantage of this method is that the beam from F2 is moved purely in translation i.e. it remains parallel to its nominal direction, and this allows the position and angle parts of the control law to be better separated & thus simplified. However this scheme still has higher-order corrections necessary. Its disadvantage is that F1 & F2 together are a larger item, and can no longer be moved using a gimbal mount. The angle control of the beam is done by tip-tilt adjust of F3, as in the previous scheme.

Control of beam for fov.
In plane of diagram.
The steering in angle & position are made by combined 'walking' of rooftop fold_1+fold_2 & fold_3 to generate the correct output pupil.

The rooftop is moved down in Y through Y_{roof}, and the 3rd mirror F3 rotated anti-clockwise, by $\alpha_3/2$.

To first order (i.e. for small fov angle α_1):
$$Z_0 = fov\_rad * F_{TEL}$$

$$\alpha_1 = Z_0/L_{PUP}$$

where fov_rad is the required field of view radius (4 arcmins), F_{TEL} is the telescope focal length (28.5m), L_{PUP} is the secondary mirror to SPIRE input focal point.

Dimension Z_1 is given by

$$Z_1 = \alpha_1.(L_{PUP}-L_{WORK})$$
$$=> Y_{roof} \sim Z_1/2 \quad \text{(exact at 45 deg)}$$

And

$$\alpha_3 = \alpha_1/2$$

in the small-angle approximation, where L_{F2F3} is the distance from mirror F2 to mirror F3.

In fig.1. $L_{F2F3} = 250$mm, the same for the other fold mirror separations, adequate for handling the beam size at 45 degree incidence.

$$L_{WORK} = R_{SM} - (L_{M2F1}+L_{F1F2}+L_{F2F3})$$

Perpendicular to plane.
To generate the FOV in the other axis, i.e. that perpendicular to the plane of the diagram (X-axis). The roof-top is rotated about Z. This generates an X-offset X_{roof} in the beam, but keeps direction unchanged. The angle θ required is given by

$$X_{roof} = L_{roof}.\tan.\theta$$

SPIRE

Technical Note

Ref:	SPIRE-RAL-NOT-000 622
Issue:	Draft Issue 1.0
Date:	08-05-2001
Page:	27 of 35
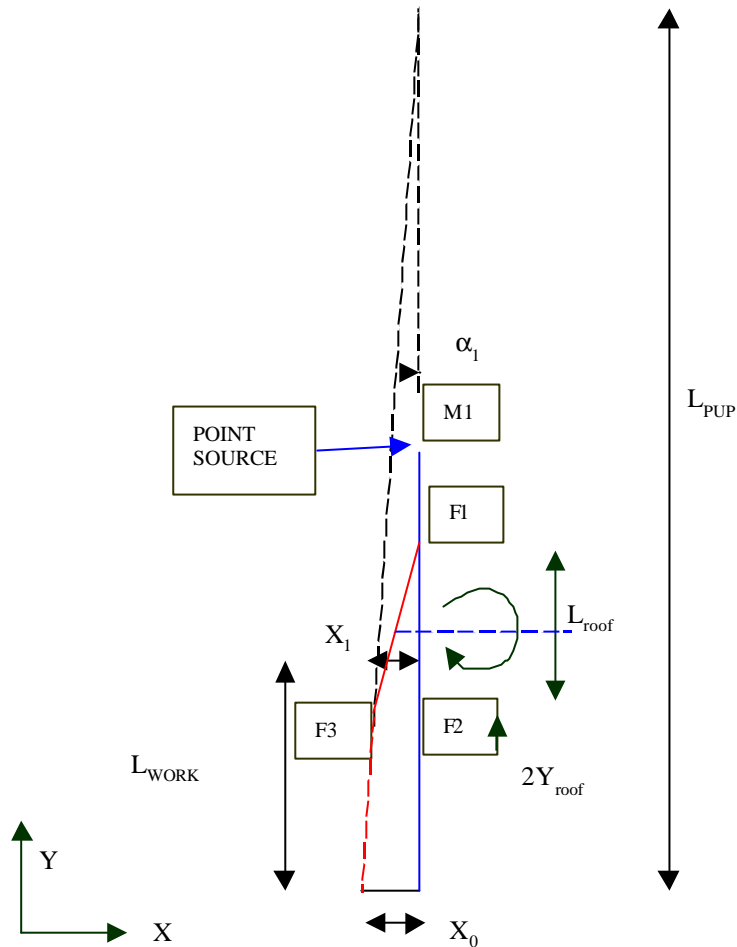
But L_{roof} changes with Z-fov.

Dimension X_1 is given by

$$X_1 = \alpha_1.(L_{PUP}-L_{WORK})$$
$$\Rightarrow X_{roof} \sim X_1 \quad \text{(exact at 45 deg)}$$

And

$$\alpha_3 = \alpha_1/2$$

Focus control: as for previous scheme.

Design Status.
The original scheme for the control laws is the baseline one. The limited range of available actuators has led to constraints on the mirror separations, fed into the overall design. These are described in reference A1.

A detailed ray-trace simulation of the 1st-order laws has been set up in Zemax, to investigate the errors, which result and determine whether higher-order correction will be necessary. The main conclusions are:
1. A linear set of actuator positions will generate a distorted (i.e. non-uniform) grid of points in beam angle space. This is acceptable for PSF measurements.

2. Some error will occur in lateral position of test-beam pupil relative to SPIRE entrance pupil nominal positions. This is zero at centre of FOV & increases towards the corners, where in the worst case it is ~ 1mm (in lateral position at Herschel M2). As this is approx 1/300 = 0.3% of the beam diameter this error is acceptable.

In view of these results (ref.A2) the first-order control laws for FOV position are accepted without higher order correction. However the function of focus control still needs to be included.

Refs.

A1. T W Grundy "Constraints on optical bench layout due to fold mirrors", 21-3-01
A2. T W Grundy "Telescope simulator control laws, steering model", 26-3-01.

Annex 2. Filters & ghosting.

The figure below shows the design with 4 elements added.
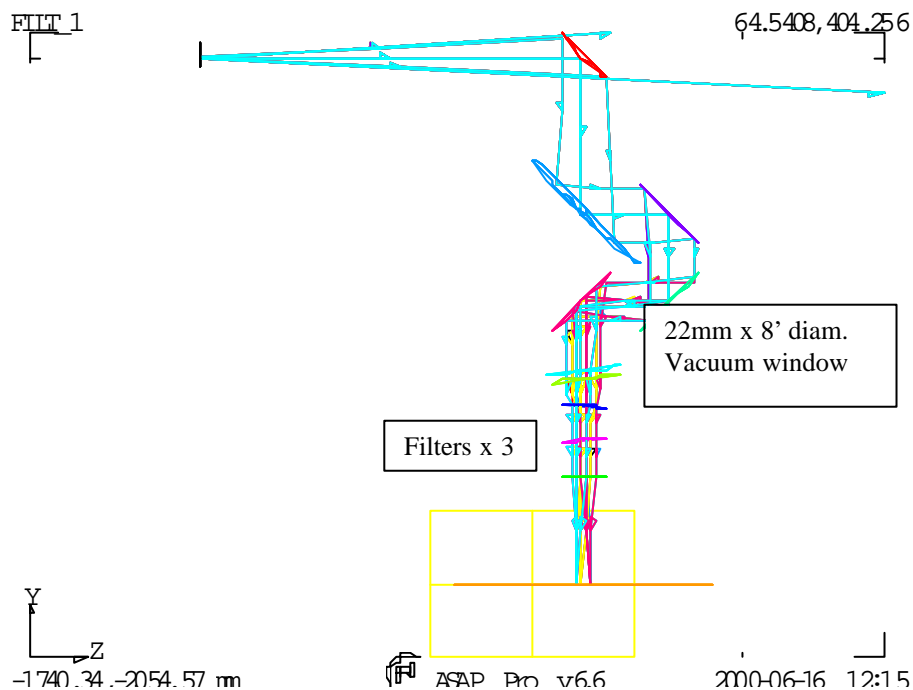
Due to the possible multiple reflections between elements, it is necessary to tilt the filters such that none of the double-bounce reflections can pass the instrument field stop. In the 1st-cut scheme shown, the elements are spaced 100mm apart (this may need to be adjusted for mechanical design). The final filter is un-tilted & the other two are tilted in opposite sense. Finally the window is tilted, by twice the amount of the filters, to prevent filter-window ghosts. The tilts are mainly about the X –axis (the inner surface of the cryostat window id also rotated about the Z-axis) so that the FOV is shifted in the direction of its narrower side (see later figure).

The figure below shows the example of a reflection between the last 2 filters, causing a defocused beam to arrive at the Field stop aperture.

SPIRE

Technical Note

Ref:	SPIRE-RAL-NOT-000 622
Issue:	Draft Issue 1.0
Date:	08-05-2001
Page:	29 of 35

FILT_1   76.6821,412.526

Y
└──► Z
−1740.34,−2062.84 mm   ASAP Pro v6.6   2000−06−16 11:57

One ghost path
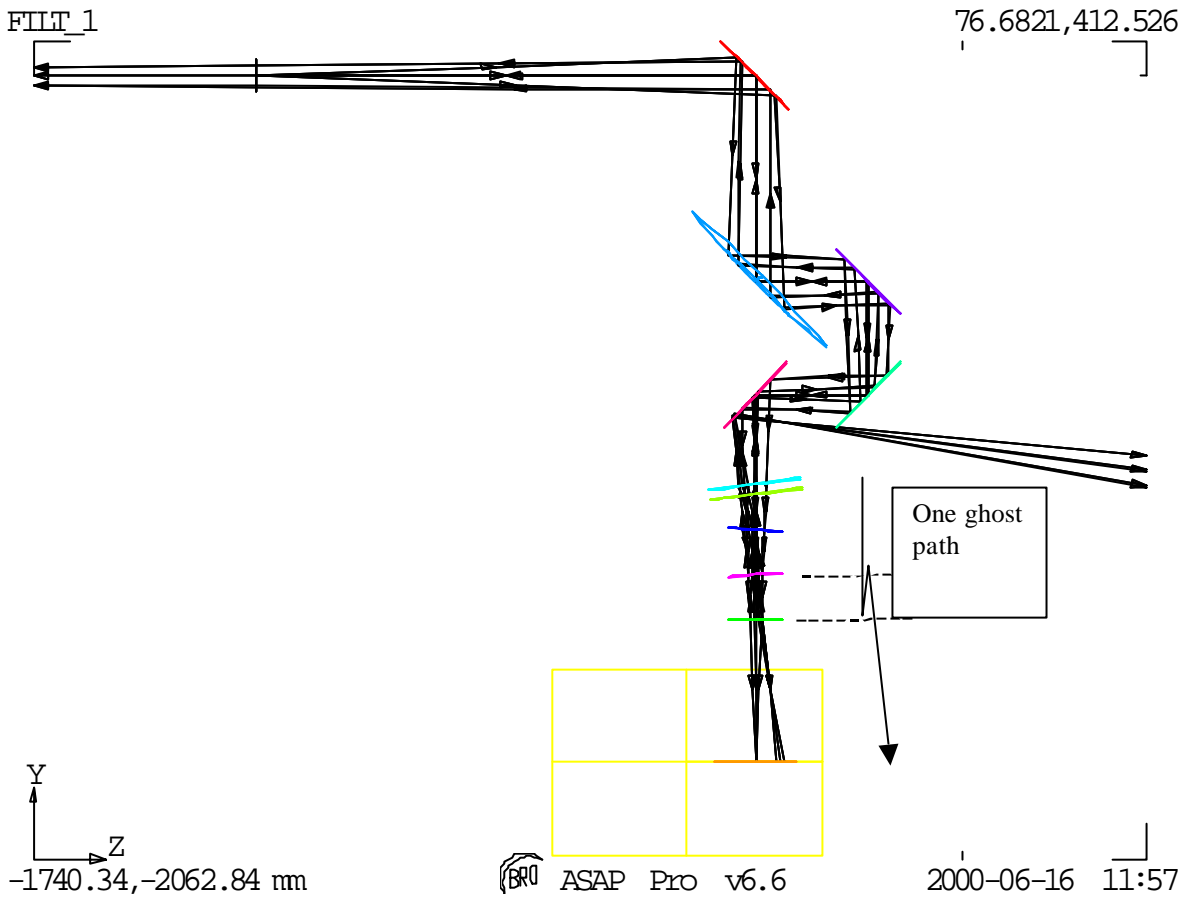
NB: filter positions have been updated since this plot, see subsequent figures below.

The simplest (but perhaps overkill) arrangement is to tilt the elements such that the whole of SPIRE's FOV is shifted by its own width. In that case, for any incident beam the ghost beams are all outside of the FOV. For the 4 partly reflecting surfaces there are 5 double-bounce reflections, leading to 5 ghost images (next figure). The full ray-trace of these & resulting field-stop plane spot diagram is shown in the next figure, for the case of the new filter positions.

TELE_SIM   2027.8,-1168.99

Y
↑
→ -Z
-202.222,1869 mm   ASAP Basic v7.0   2001-03-29 12:22

Tel. Sim.: ray impacts including from ghost reflections   -582.643,740.558

filters / filters

window back / filters

window back / window front

window front / filters

-X
↑
→ Z
582.644,-846.935 mm   ASAP Basic v7.0   2001-03-29 12:22

Here the wanted beams are those in the well-focused rectangle at the field stop. The 5 ghost reflections are defocused & are all outside of the main image as required.

This design is intended to minimise the tilt angles of the spectral filters, and uses a tilt value given by

$$\delta = atan[(2Y_0 + margin)/L_{work}')/2$$

where L_{work}' is the distance from last tilted filter to the field stop, and margin =3mm here.

This gives filter tilt of 3.4 degrees (6.8 degrees for the window).

Note that in this scheme there are reflections that pass back into the simulator & into the source, and the design may need to be refined to mitigate these.

Filter sizes

Below are displayed the beam footprints on the different surfaces (filters, cryostat window) for filters size pupose. These footprints are obtained by slicing, at theses different tilted surfaces, a tube (20% oversized for diffraction), which stands as the rays envelope for all fov positions.
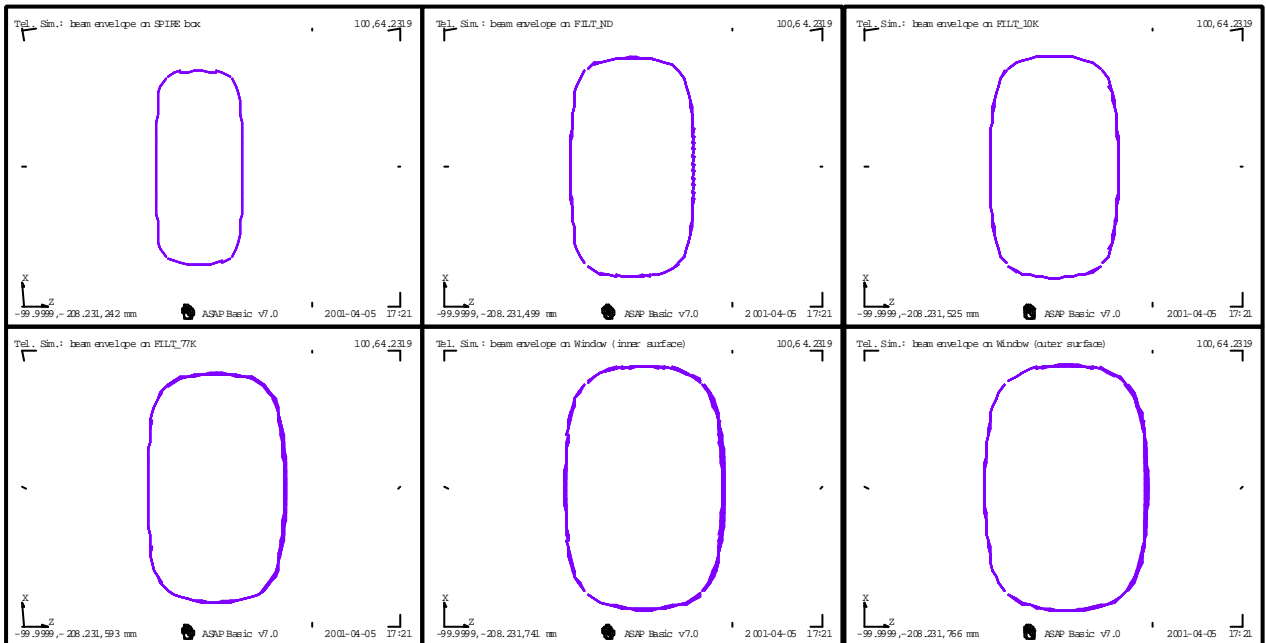
Annex 3. Flip mirror & black body.

The flip mirror & black-body surface have been added to the model along with updated filter positions, and a change to make the source enter from the opposite side of the bench to previously. The updated geometry is shown in the figure below.

FOLD_1   64.5408,-2014.96

750 tank radius

Window   77K edge filter
              10K edge filter
              ND filter (4K)

Black plate   Flipper mirror

Tank centreline

Y
-Z
-1740.34,443.859 mm   BRO ASAP Pro v6.6   2000-09-25 10:19
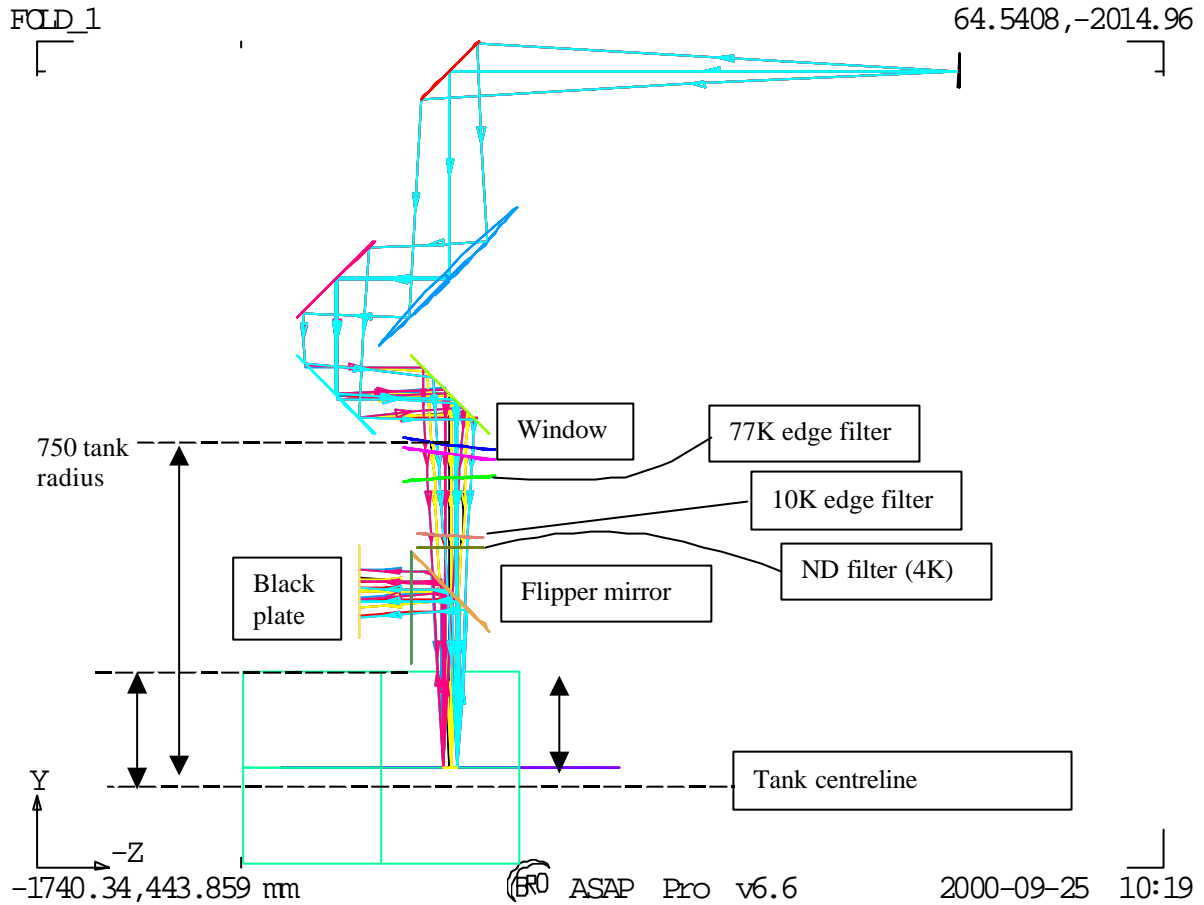
The figure shows the simulator in plan view, with the black body path flipped horizontally in Y-Z plane. The blackbody-input direction is then along the tank axis, avoiding the wall-curvature problem.

Annex 4. Beam profile due to reflective pupil mask.

In the case where a 45-degree tilted reflective pupil mask has to be considered, the beam profile in the tilted direction becomes non-ideal compared to the Herschel top-hat like profile. The tilt produces a 'ripple' at the pupil edges, to the extent shown in the simulations below.

SPIRE

Technical Note

Ref:	SPIRE-RAL-NOT-000 622
Issue:	Draft Issue 1.0
Date:	08-05-2001
Page:	33 of 35

FOLD_1

ENE Complex FIE for Z=-458

Beam profile 0.5mm wavelength, 45 deg AOI on mask.
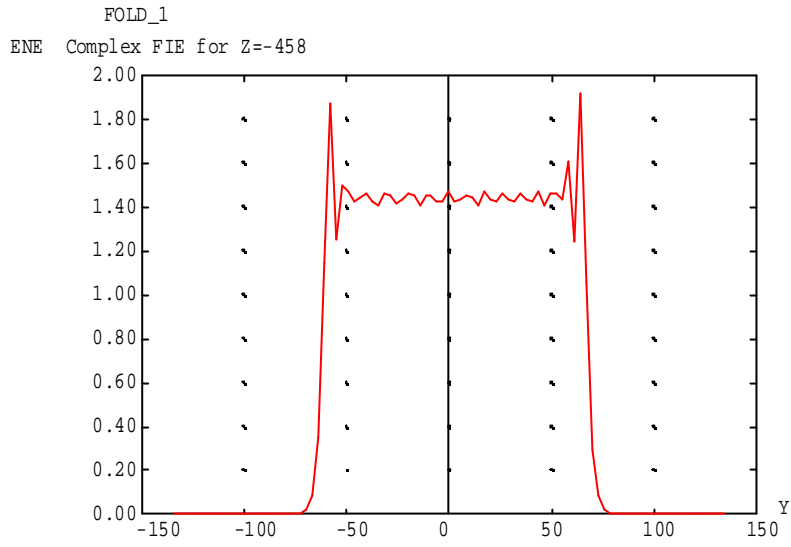
ASAP Pro v6.6   2000-10-27 16:56

FOLD_1

ENE Complex FIE for Z=-458
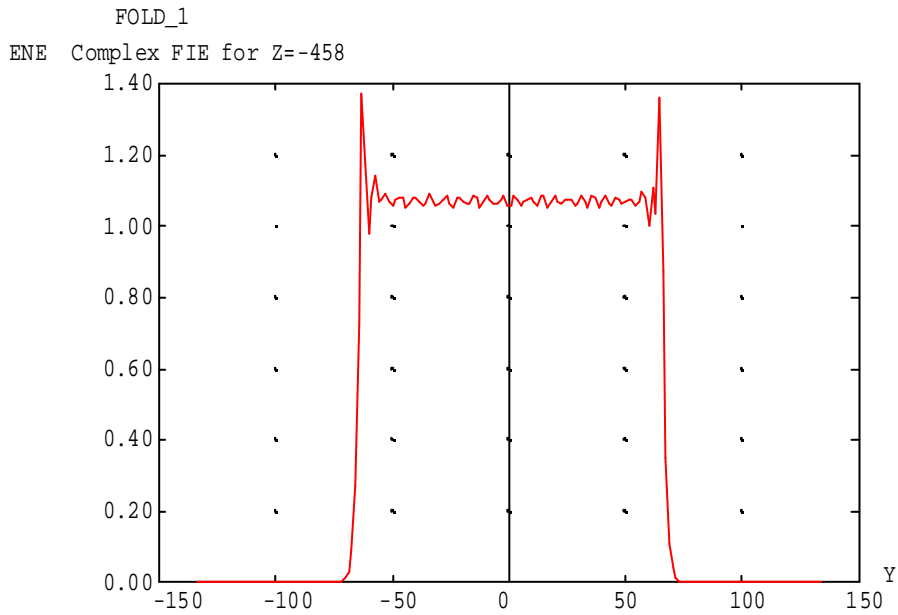
ASAP Pro v6.6   2000-10-27 17:02

AOI reduced to 20 deg.

Annex 5. Details of simulator bench layout

Constraint of space within the clean room test lab may lead to use of an optical bench with the following dimensions: length=2500 mm, width=1100 mm. The overall size of the telescope simulator system is set by the parameter R_{SM}. A possible configuration of the telescope simulator optical components, with R_{SM}=2100 mm, is displayed below in Figure xx (respecting the telescope F# and using a 1:1 imaging mirror and the entrance pupil mask used in transmission). It includes a beam-splitter for beam measurement check before entering the cryostat, located on the bench between F3 and the first cryostat window.
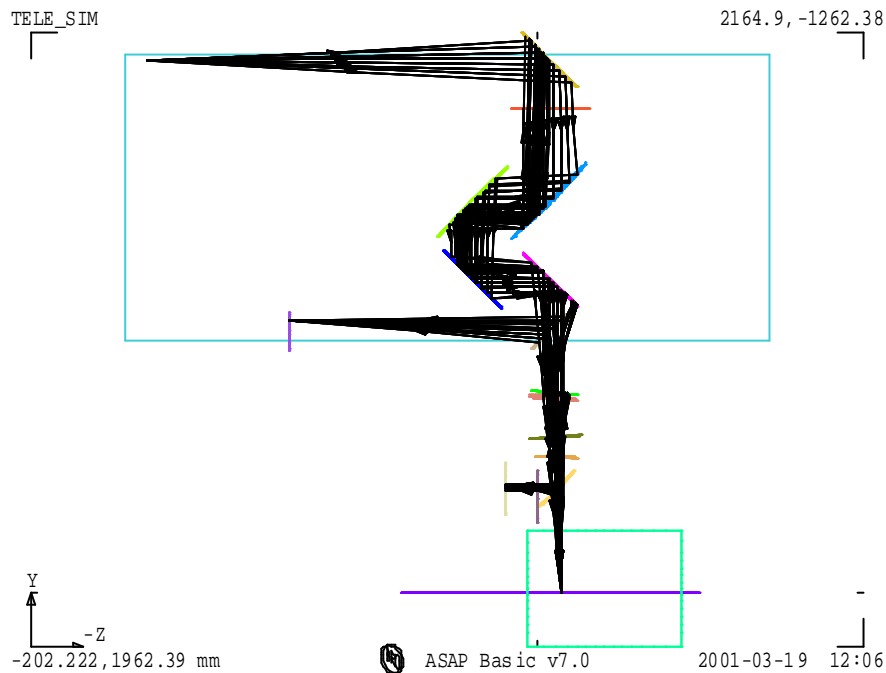
Possible layout (plan view) of the optical bench with one point-source and R_{SM}=2100 mm.

The dimensions of most optical components are also dependent on the R_{SM} value. Possible reduction of R_{SM} can be set thanks to reduction of the L_{WORK} distance (between F3 and the SPIRE input focal plane). An analysis (see A1 and A2) of the consequences of modification to L_{WORK} shows the needs to increase the distance between F2 and F3 (DF2F3), in order to keep the fold mirrors control laws, if L_{WORK} (as R_{SM}) is decreased. To avoid a another modification of L_{WORK} by the required increases in DF2F3, the path length from the imaging mirror M2 to F3 is chosen to be constant in every case, DF1F2 is then reduced (which helps accommodating the components along the short bench width) to compensate increasing DF2F3.

The possible source of reduction for L_{WORK} comes from the distance between the cryostat and the optical bench, limited by the requested presence of the beam-splitter. Figure 2 below shows an extreme case of reduction for R_{SM} leading to a value of 1920 mm. In order to be still able to simulate the Hershel space telescope pupil distance, the path length between the pupil aperture mask and M2 is increased (nearly linear variation, for the range of interest in R_{SM} values, with respect to decreases in DM1, the distance between the source and the mask). For this low value of R_{SM} and given the optical bench width, the beam would then need to be folded between the mask (assuming transmission mode,

see Annex 4 for details of field distribution degradation in case of a reflective mask) and M2 in order to keep the mask on the bench. Such a reduction in R_{SM} (and therefore in DM1) is associated with the reduction in the pupil mask diameter D1. The parameter D1 is also set by the constraints by: $D1=n*\lambda_{max}/OSC$, where $n>>1$ (typically n must be larger than 10 to avoid too large diffraction effects, see R1). Taking $\lambda_{max}=0.6$ mm, and for the range of R_{SM} values studied, the parameter n varies between 25 and 35, which remains in a safe range regarding diffraction.
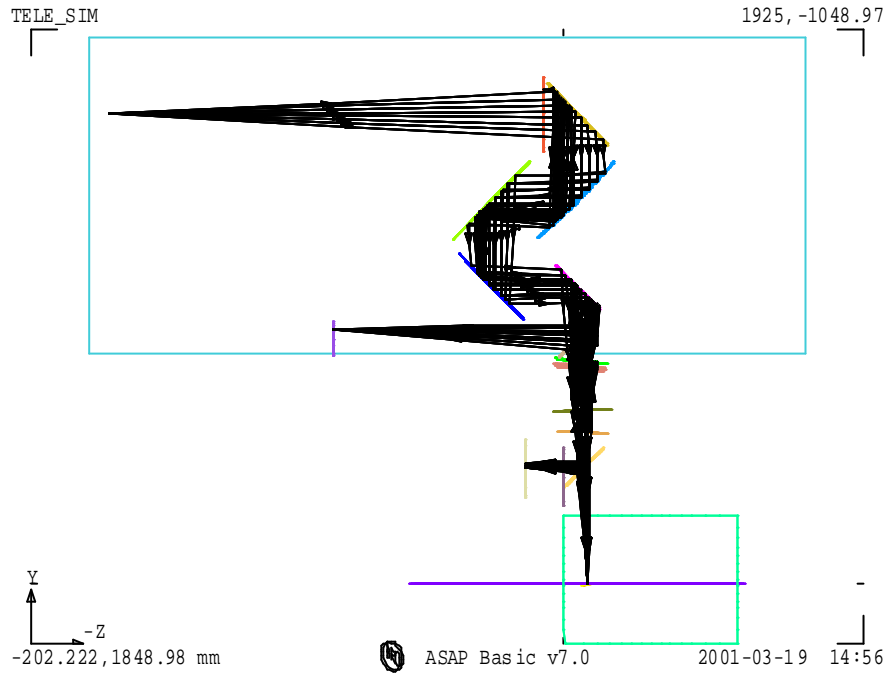
Possible layout (plan view) of the optical bench with one point-source and R_{SM}=1920 mm.